Ecological Modelling 220 (2009) 2009–2023

Contents lists available at ScienceDirect

Ecological Modelling

journal homepage: www.elsevier.com/locate/ecolmodel

A hierarchical analysis of terrestrial ecosystem model Biome-BGC: Equilibrium analysis and model calibration

Weile Wang[a,b,*], Kazuhito Ichii[c], Hirofumi Hashimoto[a,b], Andrew R. Michaelis[a,b], Peter E. Thornton[d], Beverly E. Law[e], Ramakrishna R. Nemani[b]

[a] California State University, Monterey Bay, Seaside, CA, USA
[b] NASA Ames Research Center, Moffett Field, CA, USA
[c] Faculty of Symbiotic Systems Science, Fukushima University, Japan
[d] Oak Ridge National Lab, Oak Ridge, TN, USA
[e] Department of Forest Ecosystems and Society, Oregon State University, Corvallis, OR, USA

ARTICLE INFO

Article history:
Received 12 June 2008
Received in revised form 23 March 2009
Accepted 27 April 2009
Available online 18 June 2009

Keywords:
Terrestrial ecosystem
Biome-BGC
Hierarchical analysis
Equilibrium analysis
Model calibration

ABSTRACT

The increasing complexity of ecosystem models represents a major difficulty in tuning model parameters and analyzing simulated results. To address this problem, this study develops a hierarchical scheme that simplifies the Biome-BGC model into three functionally cascaded tiers and analyzes them sequentially. The first-tier model focuses on leaf-level ecophysiological processes; it simulates evapotranspiration and photosynthesis with prescribed leaf area index (LAI). The restriction on LAI is then lifted in the following two model tiers, which analyze how carbon and nitrogen is cycled at the whole-plant level (the second tier) and in all litter/soil pools (the third tier) to dynamically support the prescribed canopy. In particular, this study analyzes the steady state of these two model tiers by a set of equilibrium equations that are derived from Biome-BGC algorithms and are based on the principle of mass balance. Instead of spinning-up the model for thousands of climate years, these equations are able to estimate carbon/nitrogen stocks and fluxes of the target (steady-state) ecosystem directly from the results obtained by the first-tier model. The model hierarchy is examined with model experiments at four AmeriFlux sites. The results indicate that the proposed scheme can effectively calibrate Biome-BGC to simulate observed fluxes of evapotranspiration and photosynthesis; and the carbon/nitrogen stocks estimated by the equilibrium analysis approach are highly consistent with the results of model simulations. Therefore, the scheme developed in this study may serve as a practical guide to calibrate/analyze Biome-BGC; it also provides an efficient way to solve the problem of model spin-up, especially for applications over large regions. The same methodology may help analyze other similar ecosystem models as well.

1. Introduction

Climate change due to anthropogenic increases in greenhouse gases has lead to concerns about impacts on terrestrial ecosystems, and has generated an imperative for the understanding of, and the ability to predict, the role of terrestrial ecosystems in the global carbon cycle (IPCC, 2007). In response to this call, a variety of biogeochemical ecosystem models have been developed since the 1980s, including CASA (Potter et al., 1993), CENTURY (Parton et al., 1993), TEM (Raich et al., 1991; McGuire et al., 1992), BGC (Running and Coughlan, 1988; Running and Gower, 1991), and many others. These models are driven by surface climate variables, and employ algorithms to simulate important ecosystem processes such as the exchange of water between the surface and the atmosphere through evaporation and transpiration, the assimilation and release of carbon through photosynthesis and respiration, and the decomposition of organic matter and the transformation of nitrogen in soil. As such, they provide an important means to simulate regional and global carbon/water cycles, and to assess the impacts of climate variability and its long-term change on these cycles (e.g, Randerson et al., 1997; Cramer et al., 1999; Schimel et al., 2000; Nemani et al., 2003).

Early versions of biogeochemical models usually have simple structures; as models evolve to create more realistic simulations, their later versions become increasingly sophisticated. For example, in Forest-BGC, the first member of the BGC family, leaf area index (LAI) of the vegetation canopy is prescribed, and carbon allocation is solely controlled by external parameters (Running and Coughlan, 1988). In the latest BGC model (Biome-BGC, version 4.2), in contrast, LAI is dynamically simulated and updated at daily scales

* Corresponding author at: c/o Ramakrishna R. Nemani, Mail Stop 242-4, NASA Ames Research Center, Moffett Field, CA 94035, USA. Tel.: +1 650 604 6444; fax: +1 650 604 6569.
E-mail address: weile.wang@gmail.com (W. Wang).

0304-3800/$ – see front matter © 2009 Elsevier B.V. All rights reserved.
doi:10.1016/j.ecolmodel.2009.04.051

with an integrated consideration of both carbon and nitrogen fluxes (Thornton et al., 2002). The current Biome-BGC also treats litter and soil processes in much detail, simulating the transformation of carbon and nitrogen between four different litter pools and four different soil pools (Thornton and Rosenbloom, 2005; Thornton, 1998). (The latest Biome-BGC model and its documentation are available online at http://www.ntsg.umt.edu.)

An indicator of a model's complexity may be the number of parameters that are used in the model to characterize various ecosystem processes or to represent different environmental properties. Currently, the core algorithm of Biome-BGC requires 67 parameters to be specified, of which 23 parameters are assumed constant model-wide, 34 parameters are specific to the plant functional type (PFT), and 10 parameters are specific to the study site. Determining appropriate values for these parameters requires great diligence: White et al. (2000) represents 40 pages of referenced source data to calculate a default set of ecophysiological parameters for Biome-BGC (which are supplied with the distribution of the BGC model). Still, these default parameters are intended for general guidance only: for a model as complex as Biome-BGC, small uncertainties in the parameters may propagate to generate a wide range of variability in the subsequent simulations, and thus model parameters need to be fine tuned for particular applications.

Because ecosystem processes tend to be nonlinear, numerical inversion algorithms are usually adopted for parameter tuning. These algorithms generally define a cost function that measures the mismatch between model simulations and the corresponding observations, and search for a set of "optimal" values that minimize the cost function. For instance, a search process usually starts with examining how the cost function responds to small changes in the parameters of interest; it then uses this information to determine new parameter values that decrease the cost function: the procedure is repeated until the minimum of the cost function is reached. Applications and reviews of typical inversion algorithms used in ecosystem model calibration can be found, for instance, in Wang et al. (2001, 2006), Knorr and Kattge (2005), Williams et al. (2005), and Raupach et al. (2005).

There are a few difficulties, or limitations, associated with the inversion of complicated models. First, because the search for an optimal solution is an iterative process, the inversion procedure may consume lots of processing power when the model is complicated and there are many parameters to calibrate (Wang et al., 2001; Raupach et al., 2005). Second, deciding the subset of parameters for calibration itself can be a difficult process. With the computation costs considered, generally we would like to calibrate parameters that are important and mutually independent (Harmon and Challenor, 1997). However, parameters (and the processes they characterize) in complex models preclude easy determination of the relative importance and independence of their component parts. Finally and most importantly, numerical inversion algorithms treat the ecosystem model as a "black-box" process, in which only the tested relationships between inputs (i.e., changes in parameters) and outputs (i.e., usually a few selected variables for which observations are available) are used. Thus the retrieval of optimal parameter values does not necessarily help with insight into the physical processes represented by the model. There are occasions in which we may be more interested in understanding why and how (rather than knowing what) certain values of parameters render the most realistic simulations. Numerical algorithms alone cannot fully address these questions.

Altogether, as today's ecosystem models strive to create more realistic simulations, their increasing complexity induces a major difficulty in tuning parameters and analyzing results, which in turn limits the application of the models themselves. To address this problem, on one hand, simplifications are necessary; on the other hand, the simulation capacity of the models should not be impaired. This creates a dilemma that is faced by anyone seeking to use modern ecosystem models.

Held (2005) discussed a similar dilemma for climate modeling. As suggested by Held (2005), a general solution to problems of this kind relies on the construction of model hierarchies. For instance, suppose there is a set of models that are coherently related to, but less complex than, the model we are working on. By comparing the behavior of the original complex model to that of simpler ones, we can gain understanding of "how the dynamics change as key sources of complexity are added or subtracted" (Held, 2005). Also, parameters can be first tuned on simpler models, and then applied to more complicated systems.

The set of coherently related models (including the original one) that have different levels of complexity forms a "model hierarchy" (Held, 2005). For most ecosystem models, such a model hierarchy is not be readily available, but may be constructed by sequentially removing certain functional components from the original model. Motivated by this approach, in this study we develop a model hierarchy for Biome-BGC and demonstrate its application in model analysis and parameter tuning at four AmeriFlux sites.

The rest of the paper is structured as follows. Section 2 describes the methodology and the dataset. The hierarchical scheme is then applied to analyze and calibrate Biome-BGC at four AmeriFlux sites, and the results are represented and discussed in Section 3. Finally, Section 4 gives the concluding remarks.

2. Methodology and datasets

2.1. Model hierarchy and equilibrium analysis

With a focus on the carbon cycle, we identify three key functional tiers in Biome-BGC: (1) photosynthesis and evapotranspiration at the leaf level; (2) carbon (and nitrogen) allocation and respiration at the whole-plant level; and (3) carbon/nitrogen cycles in litter/soil pools (Fig. 1). The three functional tiers also have a timescale component to them, with photosynthesis and ET being the fast processes and the first processes whereby carbon enters (and water leaves) the ecosystem, while carbon and nitrogen cycles in litter/soil pools being the slowest processes that depend on the other two tiers (Williams et al., 2005). For simplicity of the text, here we give a qualitative introduction to the derived model hierarchy, but leave detailed mathematic derivations in Appendix B. Tables 1a–1c lists abbreviations and symbols that are frequently used in the following sections.

Photosynthesis (PSN) and evapotranspiration (ET) are two closely related processes that occur at the leaf level (Fig. 1a). PSN represents the start of the carbon cycle in Biome-BGC, which assimilates atmospheric CO_2 into the ecosystem (measured by gross primary production, GPP); during the same process, water is transpired from the soil to the atmosphere. In Biome-BGC, both

Table 1a
List of frequently used abbreviations.

Abbreviation	Description
PSN	Photosynthesis
GPP	Gross Primary Production
NPP	Net Primary Production
NEE	Net Ecosystem Exchange
MR	Maintenance Respiration
GR	Growth Respiration
AR	Autotrophic Respiration
HR	Heterotrophic Respiration
PFT	Plant Functional Type
ENF	Evergreen-Needle-leaf Forest
DBF	Deciduous Broadleaf Forest
LAI	Leaf Area Index
SLA	Specific Leaf Area

Table 1b
List of model parameters/state variables.

Symbol	Units	Description
α_{lf}	1/yr	Annual leaf and fine root turnover fraction
α_{wd}	1/yr	Annual live wood turnover fraction
β_{age}	1/yr	Annual whole-plant mortality fraction
β_{fire}	1/yr	Annual fire mortality fraction
r_1	(0–1)	Allocation ratio—new fine root C:new leaf C
r_2	(0–1)	Allocation ratio—new stem C:new leaf C
r_3	(0–1)	Allocation ratio—new live wood C:new total wood C
r_4	(0–1)	Allocation ratio—new coarse root C:new stem C
d_{eff}	m	Effective soil depth
f_{lnr}	(0–1)	Fraction of leaf nitrogen in Rubisco
f_{pi}	(0–1)	Fraction of actual immobilization (of soil mineral nitrogen) to potential immobilization
$g_{s,max}$	$m\,s^{-1}$	Maximum stomatal conductance
C_x	$kg\,C/m^2$, $kg\,C/m^2/s$	Carbon stock or carbon flux specified by the subscript
N_x	$g\,C/m^2$, $g\,C/m^2/s$	Nitrogen stock or nitrogen flux specified by the subscript
$C{:}N_x$	Ratio	Carbon–nitrogen mass ratio

processes are calculated on a basis of projected leaf area—they can be fully calculated if the leaf area of the canopy (represented by leaf area index or LAI) is known. Therefore, if we prescribe LAI but remove the rest of carbon/nitrogen cycles from the model, it should still be able to simulate GPP and ET. Such a simple land-surface scheme defines the first model in our hierarchy (referred to as the "first-tier" model).

GPP simulated by the first-tier model provides the primary carbon input for the plant-level carbon cycle (Fig. 1b). In particular, GPP less maintenance respiration (MR) represents carbon that is available for allocation, which potentially can be all allocated to different vegetation tissues based on the allometric relationships among them (prescribed as model parameters). Accompanying the allocation of carbon, a certain amount of nitrogen must also be allocated to vegetation tissues so that their C:N ratios (prescribed as model parameters) are maintained. Therefore, the actual allocation is not only determined by available carbon, but also regulated by the amount of available nitrogen (mainly N uptake from the soil). Normally, the determination of N uptake involves complicated calculations of soil/litter processes; however, if we are able to estimate carbon allocation and N uptake alternatively from *a priori* information (e.g., measurements of NPP, litter production rate, and so on), these soil/litter processes may be ignored. Therefore, by removing soil/litter processes from the original Biome-BGC, the second model is defined in our hierarchy (referenced as the "second-tier" model). Compared with the first-tier model, the second-tier model incorporates carbon/nitrogen cycles at the plant level, so that the growth of vegetation (LAI, in particular) is now dynamically simulated instead of being prescribed.

Finally we examine carbon/nitrogen cycles in litter and soil pools (Fig. 1c). Per Biome-BGC algorithms, dead vegetation tissues (via turnover or whole-plant mortality) are decomposed through a series of stages and at varying rates, which are represented by multiple litter pools and multiple soil pools (although for simplicity, Fig. 1(c) shows only one litter pool and one soil pool, respectively). In general, organic matter flow from fast-decaying pools (e.g., litter) to slow-decaying pools (e.g., soil), during which a proportion of carbon is released to the atmosphere through heterotrophic respiration (HR). The cycling of nitrogen is a bit more complicated: depending on the C:N ratios of the organic matter and its destined pool,

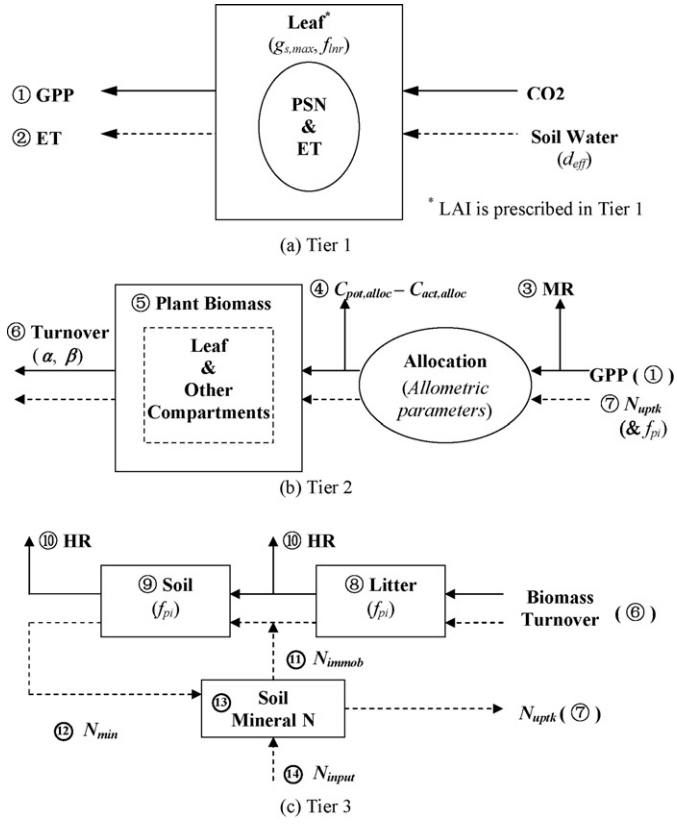

Fig. 1. Schematic diagrams of the proposed hierarchy of Biome-BGC, shown as being analyzed in model calibration. The three tiers respectively describe (a) photosynthesis (PSN) and evapotranspiration (ET) at leaf level; (b) carbon and nitrogen cycles at whole-plant level, and (c) carbon and nitrogen cycles in soil and litter pools. Symbols and abbreviations are explained in Tables 1a–1c, and the numbers (e.g., ①, ②, ...) indicate the order in which the major carbon/nitrogen fluxes are determined through the calibration process.

Table 1c
List of symbols for ecosystem compartments.

Symbol	Ecosystem compartment
lf	Leaf
fr	Fine root
lst	Live stem
dst	Dead stem
lcr	Live coarse root
dcr	Dead coarse root
cwd	Coarse woody debris
*litr*1	Litter—labile proportion
*litr*2	Litter—unshielded cellulose proportion
*litr*3	Litter—shielded cellulose proportion
*litr*4	Litter—lignin proportion
*soil*1	Soil—fast microbial recycling proportion
*soil*2	Soil—medium microbial recycling proportion
*soil*3	Soil—slow microbial recycling proportion
*soil*4	Soil—recalcitrant (slowest) proportion

Table 2a
Site information: general information.

Site Name (Code)	Symbol	Location	Veg. type[a]	Period	References
Metolius Intermediate Pine, OR (US-Me2)	MT	44.45, −121.56	ENF	2002–2004	Law et al. (2003)
Niwot Ridge, CO (US-NR1)	NR	40.03, −105.55	ENF	2000–2004	Monson et al. (2002)
Morgan Monroe State Forest, IN (US-MMS)	MM	39.32, −86.41	DBF	2000–2004	Schmid et al. (2000)
Willow Creek, WI (US-WCr)	WC	45.91, −90.08	DBF	2000–2004	Cook et al. (2004)

the decomposition process may release surplus nitrogen (mineralization) or may require extra nitrogen (immobilization). Note that the total soil mineral nitrogen may be lower than that potentially demanded by immobilization and vegetation N uptake: in this case, the actual immobilization and the actual uptake will be prorated. Indeed, it is the central task of simulating all soil/litter processes to estimate the balance among nitrogen mineralization, immobilization, and N uptake. Therefore, the last model in our hierarchy (referred to as the "third-tier" model) is defined by incorporating the litter/soil processes to the second-tier model. The third-tier model is the original, complete version of Biome-BGC.

To simplify the analysis of the proposed model hierarchy, this study considers a special status of models, that is, when they are at "equilibrium". Generally, equilibrium of an ecosystem model refers to a steady status in which model state variables reach a dynamical balance (e.g., dead tissues are replaced by new tissues of the same quantities) so that they do not change at annual or longer time scales. In most experiments, model state variables need to be first "spun up" into equilibrium with respect to the specified climate and ecophysiological conditions (Thornton and Rosenbloom, 2005). Ideally, if the model is spun-up using periodic meteorological data that represent the climatology of the site, the resulting state variables will have the same seasonal cycles and there will be no interannual variability in them. System equilibrium is generally approximated by the climatologies (i.e., mean seasonal-cycles) of the model state variables brought by spin-up runs.

The analysis and calibration of models can be simplified under the assumed system equilibrium. For instance, because the state variables are periodic at system equilibrium, we need to only specify the *mean* LAI cycle in the first-tier model when calibrating it against observed fluxes of ET and GPP. Furthermore, because there is no interannual variability in the state variables, they can be regarded as constant at annual (or longer) time scales. As such, the "slow" ecosystem processes (i.e., carbon allocation, soil decomposition, etc.) in the second-tier and the third-tier models can be easily analyzed with the principle of mass balance.

To illustrate, suppose we have calibrated the first-tier model such that it appropriately simulates observed ET and GPP with prescribed LAI. Now consider how to calibrate the second-tier model. Clearly, if we keep model components that are already calibrated in the first-tier model unchanged, but calibrate the other components (that deal with carbon allocation) in a way that they dynamically support a canopy with the same LAI as previously prescribed, the whole second-tier model will be calibrated.

We evaluate the above problem by applying the principle of mass balance: under the assumed equilibrium assumption, LAI of the canopy does not change year to year, and carbon annually allocated to leaf must be the same as the annual leaf-carbon loss through decay (i.e., turnover or mortality). The latter can be easily estimated because the leaf carbon stock is already known (determined by LAI and SLA, specific leaf area), and the rates of turnover and mortality are prescribed model parameters. The same approach can be extended to determine carbon stocks and fluxes for other plant components, based on their allometric relationships with leaves (all of which are model parameters). Subsequently, all major carbon (and nitrogen) fluxes in the second-tier model are derived. The analysis and calibration of soil/litter processes in the third-tier model can be simplified in the same way as above. Therefore, once the first-tier model is calibrated, the calibration of the second-tier and the third-tier models can be conducted in an analytical fashion, with no numerical inversion techniques involved. This not only simplifies model calibration in terms of computation, but also provides insight into the underlying ecosystem processes and their interactions. For the first-tier model, because its LAI is fixed, its calibration is rather easy and straightforward (see below).

Based on the derivations of the model hierarchy in Appendix B, the following results can be obtained, which provide basic guidance to analyze the model against observational data in the next section. They are:

- For the first-tier model, a set of three parameters, $g_{s,max}$ (maximum stomatal conductance), d_{eff} (effective soil depth), and f_{lnr} (fraction of leaf nitrogen in Rubisco) allows us considerable flexibility to calibrate the model against observed fluxes of ET and GPP;
- At system equilibrium, biomass of various vegetation tissues can be estimated from leaf mass by simple ratios that are fully determined by model parameters describing living-tissue turnover, whole-plant mortality, and allometric allocation;
- By comparing how much nitrogen is required by plant to allocate all available carbon and how much nitrogen is actually allocated, it helps to estimate soil nitrogen availability, and subsequently estimate various soil carbon/nitrogen pools.

2.2. Datasets

We demonstrate the application of the proposed model hierarchy to analyze and calibrate Biome-BGC at two evergreen-needle-forest (ENF) sites and two deciduous-broadleaf-forest (DBF) sites (Table 2a): the Metolius (MT) intermediate-aged pine forest in Oregon (Law et al., 2003), the Niwot Ridge (NR) subalpine conifer forest in Colorado (Monson et al., 2002), the Morgan Monroe (MM) deciduous forest in Indiana (Schmid et al., 2000), and the Willow Creek (WC) deciduous forest in Wisconsin (Cook et al., 2004). All these sites are part of the AmeriFlux networks, where fluxes of water and carbon have been systematically measured hourly (or half-hourly) since the late 1990s or early 2000s.

For all sites, we acquired hourly or half-hourly measurements of ET and GPP for the period of 2000–2004, and processed their 8-day averages as described in Yang et al. (2006). In particular, we treated missing values in the original measurements based on the procedures of Falge et al. (2001): (1) if more than 70% of data were missing in an 8-day period, this period was marked as missing; (2) if a particular time of day (e.g., 2 P.M.) was missing in all 8 days, this period was marked as missing; (3) if neither condition 1 nor 2 were met, we filled missing values with the mean from the non-missing days: for instance, if a single 2 P.M. value was missing from the 8-day period, it would be filled with the mean of the rest seven 2 P.M. values.

We also acquired site-specific biological data from the AmeriFlux website (http://public.ornl.gov/ameriflux/). This ancillary dataset, provided by investigators at each flux tower site, includes information that describes site physical characteristics, biological attributes (of vegetation, litter, and soil), as well as site disturbance

Table 2b
Site information: physical and ecological attributes.

	MT	NR	MM	WC
Elevation (m)	1253	3050	275	520
Sand (%)	67	59	34	56
Clay (%)	7	31	63	33
Silt (%)	26	10	3	11
Surface Albedo	0.26	0.26	0.20	0.20
LAI	3.4	3.6	5.0	5.4
Leaf Mass (kg C/m^2)	0.37	0.38[b]	0.22	0.18
Fine Root (kg C/m^2)	0.28	–	0.27	0.23
Wood Mass (kg C/m^2)	6.43	7.25	10.40	7.18
Leaf Production (kg C/m^2/yr)	0.07	0.11	0.21	0.15
Wood Production (kg C/m^2/yr)	0.17	–	0.32	0.15

[a] ENF, evergreen-needle-leaf forest; DBF, deciduous broadleaf forest.
[b] Inferred from LAI and site measured LMA (leaf mass per unit leaf area).

history. Yet, because the set of information may be originally collected for different purposes, the reported biological attributes are often incomplete and sometimes inconsistent at different sites due to diverse measurement approaches that were involved (although this has been remedied recently by use of standard protocols in Law et al., 2009). Based on careful evaluation, therefore, we chose six biological variables (in addition to several site physical attributes) for data-model comparison in this study, which are more consistently measured among the studying sites. They include leaf area index (LAI), leaf biomass, fine-root biomass, aboveground wood biomass, annual leaf production, and annual aboveground wood production (Table 2b). These variables are generally reported by a single value in the ancillary dataset; when multiple values are reported for a variable, its mean value (between the period of 2000 and 2004) is used. The finally compiled values of these variables (Table 2b) are consistent with previously reported in the literature (e.g., Law et al., 2003; Schwarz et al., 2004; Turnipseed et al., 2002; Curtis et al., 2002; Martin and Bolstad, 2005). For some land surface parameters (e.g., mean surface albedo) that are missing from the site-specific ancillary dataset, we filled them with values from a high resolution (1 km) global dataset, ECOCLIMAP (Masson et al., 2003).

Table 3
Parameters calibrated in the first-tier model. Values in regular-face are original parameters of Biome-BGC; values in italics indicate the calibrated parameters (shown if they are different from the original ones).

	MT		NR		MM		WC	
$g_{s,max}$ ($\times$100)	0.30	*0.20*	0.30	*0.14*	0.50	*0.25*	0.50	*0.23*
d_{eff}	1.44	*1.31*	1.04	*1.76*	0.93	*0.87*	1.52	*1.09*
f_{lnr}	0.06		0.06	*0.04*	0.08	*0.06*	0.08	*0.10*

Last, we compiled daily meteorological fields for the studying sites using the Surface Observation and Gridding System (SOGS, Jolly et al., 2005), an adaptation of DAYMET (Thornton et al., 1997). Daily maximum/minimum temperature and precipitation are interpolated based on observations from the nearest Climate Prediction Center (CPC) and National Weather Service Cooperative Observer Program (COOP) climate stations (Jolly et al., 2005). Vapor pressure deficit (VPD) and incident solar radiation are then calculated based on algorithms described in Campbell and Norman (1998). Though not shown, the SOGS data are in good agreement with gap-filled site meteorology (compiled by Dr. Daniel Ricciuto at Oak Ridge National Lab, unpublished data).

3. Results and discussion

3.1. First-tier model

The first step to analyze the first-tier model is to specify the mean seasonal cycle of LAI. This is done by rescaling the mean LAI cycles obtained from the pre-calibration model experiments (Fig. 2). For the ENF sites, the simulated LAI has little seasonal variability, and it is rescaled so that the annual mean LAI matches with site measurements (3.4 at MT and 3.6 at NR, respectively; Table 3); for the

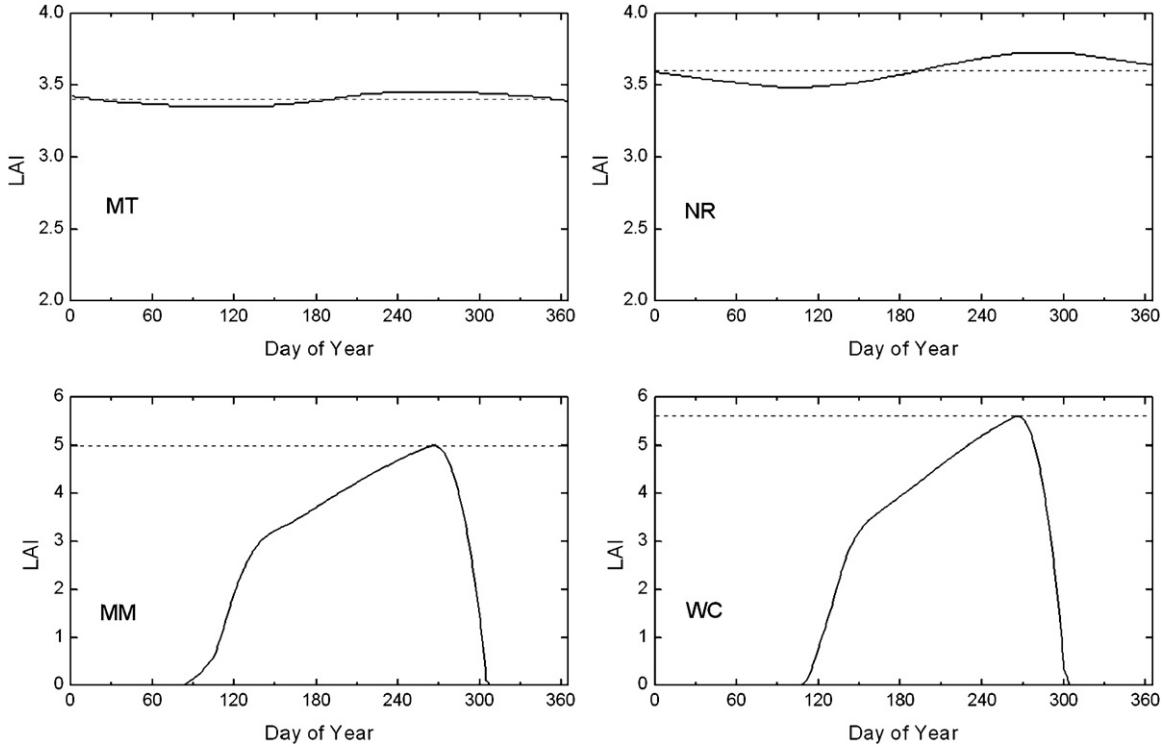

Fig. 2. Mean modeled LAI cycles prescribed in the first-tier model (solid lines). The dash lines indicate *in situ* observed annual mean or maximum LAI.

DBF sites, the mean LAI cycle is rescaled so that its peak matches with observations (5.0 at MM and 5.4 at WC, respectively; Table 3; Fig. 2).

Comparing the seasonal LAI cycles shown in Fig. 2 with other data sources (e.g., MODIS LAI product) may indicate some "unrealistic" features: for instance, modeled LAI at the two DBF sites does not really level off after it reaches a maturity point in the spring, but keeps increasing (although at a slower rate) during the growing season until senescence starts (Fig. 2). Such discrepancies reflect limitations of current Biome-BGC (and other ecosystem models in general), for the mechanisms involved in plant phenology and seasonal allocation dynamics are still poorly understood (Waring and Running, 1998). Because this kind of problem cannot be easily solved by tuning a couple of model parameters, it is not further addressed in this study. But we notice that in applications where simulations of dynamic carbon and nitrogen cycles are not necessary, it remains an option to prescribe observed LAI in the first-tier model.

We used a standard Levenberg–Marquardt algorithm (Press et al., 1992) to tune the three selected parameters (i.e., $g_{s,max}$, d_{eff}, and f_{lnr}). This algorithm searches optimal values for these parameters so that the difference (in term of squares of errors) between the simulated and the observed ET and GPP becomes least. To avoid the influence of unit differences between ET and GPP on the results, the two fluxes are normalized by their peak values, respectively. Also, to avoid lengthy iterations, the searching algorithm is set to stop when the reduction in the root-mean-square of errors (RMSE) is less than 0.1% between two successive iterations. We repeated this process with various initial values for the selected parameters, and the results consistently converge toward the same direction, indicating a stable solution for each site.

Table 3 shows the fine-tuned parameters (as well as their original values supplied with Biome-BGC), while Fig. 3 shows model simulated ET and GPP fluxes, before and after the calibration, compared with observations. As shown, at MT the first-tier model works well with original parameters, only that the magnitude of ET is a bit too high in summer (Fig. 3a). Therefore, the calibration process moderately decreased $g_{s,max}$ (Table 3). At the other three sites, ET is more distinguishably higher than observations before calibration: it usually reaches 5 mm/day in the summer, while the peaks of observed ET range between 3 mm/day (NR, WC) and 4 mm/day (MM). This led a reduction by about half in the find-tuned $g_{s,max}$ at these sites (Table 3). At NR, before calibration ET also shows an earlier decrease during the season, suggesting insufficient soil water

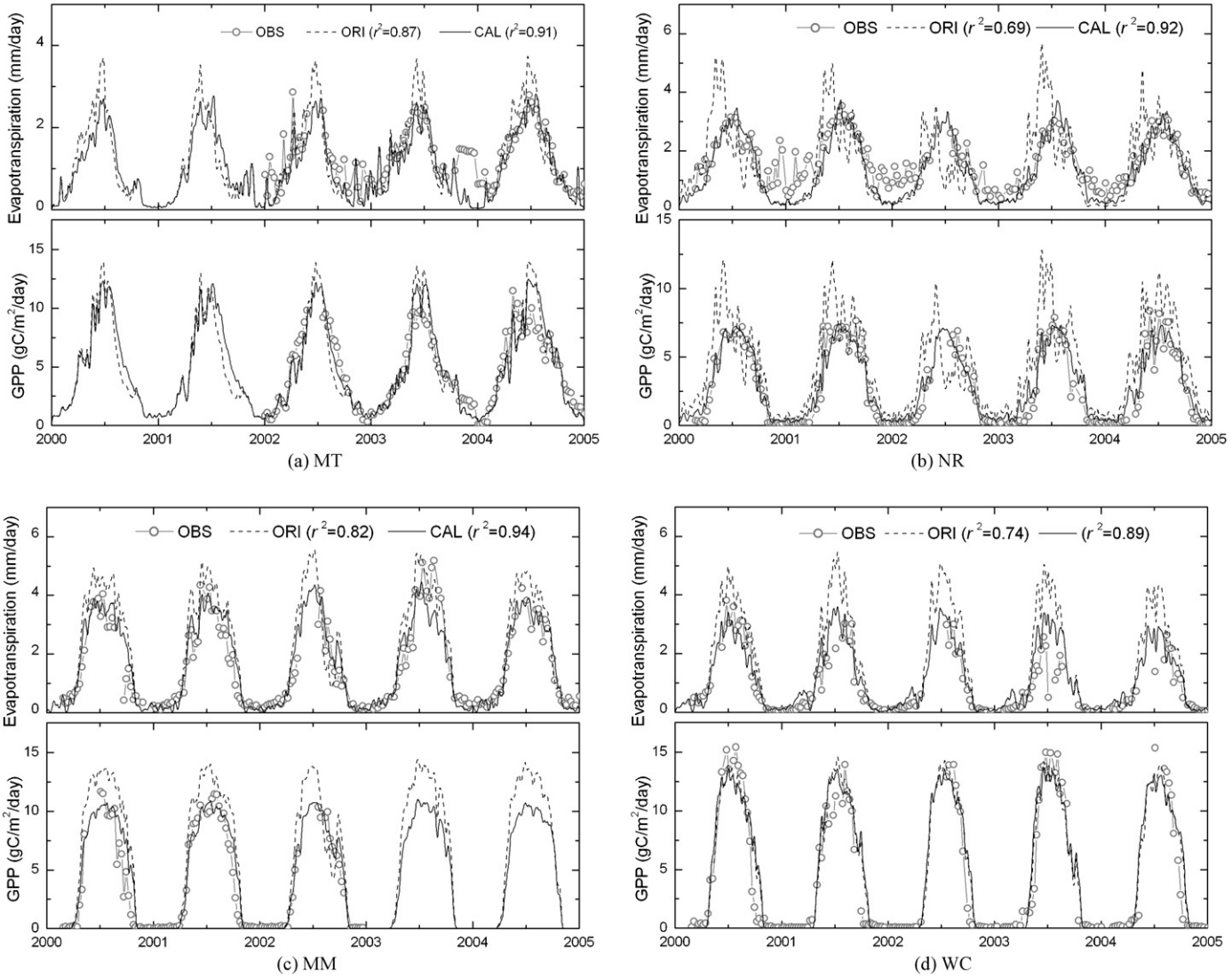

Fig. 3. ET and GPP simulated by the first-tier model with original parameters (dashed black lines; "ORI") and calibrated parameters (solid black lines; "CAL"). The gray lines ("OBS") show the corresponding tower measurements.

Table 4a
Parameters of vegetation turnover, mortality, and allocation. Values in regular-face are original Biome-BGC parameters; values in italics indicated those revised in this study.

	ENF (MT, NR)		DBF (MM, WC)	
α_{lf}	0.25		1	
α_{wd}	0.7		0.7	
β_{age}	0.005	*0.015*	0.005	*0.015*
β_{fire}	0.01		0.0025	*0.01*
r_1	1		1	
r_2	2.2		2.2	*1.5*
r_3	0.1	*0.2*	0.1	*0.2*
r_4	0.3		0.23	

Table 4b
Biomass ratios between different vegetation compartments. Values in regular-face are calculated with the original parameters; values in italics are calculated with revised parameters.

	ENF (MT, NR)		DBF (MM, WC)	
C_{fr}:C_{lf}	1		1	
C_{lst}:C_{lf}	0.08	*0.17*	0.31	*0.42*
C_{dst}:C_{lf}	38.79	*24.03*	295.22	*61.08*
C_{lcr}:C_{lst}	0.3		0.23	
C_{dcr}:C_{dst}	0.3		0.23	

capacity; as a result, the calibration process increased d_{eff} by 70% (Table 3). On the other hand, the tuned d_{eff} is decreased at MM and WC. Finally, the calibration process decreased f_{lnr} at NR and MM, but increased it at WC to make the simulated GPP match with observations (Table 3; Fig. 3).

After the calibration, model simulated ET and GPP capture about 90% variance of the observed fluxes (Fig. 3, as indicated by the r^2 statistics). Annual GPP is estimated about 1.1–1.6 kg C/m^2/year among these sites (Table 5).

3.2. Second- and third-tier models

The theoretical analysis of the second-tier model indicates that at system equilibrium, carbon storages in other vegetation tissues are related to leaf carbon by simple ratios that are determined by model parameters describing living-tissue turnover, whole-plant mortality, and carbon allometric allocation (Eq. (10) of Appendix B). Tables 4a–4c lists these parameters (Table 4a) and the estimated biomass ratios (Table 4b); it also lists a few biomass ratios that are calculated based on site observations (Table 4c).

Overall, model estimates and observations agree that the biomass of fine-root is approximately the same as the biomass of leaf (Tables 4a–4c); However, model estimates and observations are quite different for biomass ratios between stem (aboveground woody tissues, in general) and leaf: the observed stem-to-leaf ratios are about 18 at the two ENF sites and about 44 at the two DBF sites (Table 4c), while with the original parameters, the model estimated stem-to-leaf ratios are about 39 and 296 for ENF and DBF, respectively (Table 4b). Previously, Jenkins et al. (2003) investigate biomass distribution of U.S. tree species using synthesized allometric models. Interpreting the results by Jenkins et al. (2003) into the context of this study suggests stem-to-leaf ratios around 20 and 50 for mature needle-leaf trees and broadleaf trees, respectively. In Oregon, field measurements of LAI, LMA and wood biomass on 95 1-ha plots in evergreen-needle-leaf forests indicate an average stem-to-leaf ratio of 36 for forests 20–800 years old, and 22 for stands 30–50 years old; the highest values were in mature and old forests (Law et al., 2004). Therefore, the observed biomass ratios at the four studying sites (Table 4c) are consistent with the results of Jenkins et al. (2003), and suggest that the model estimated stem-to-leaf ratios may be too high. Finally, the model estimated biomass ratios between coarse root and stem is about 0.2–0.3, which are comparable to previous observational studies (e.g., Cairns et al., 1997) or allometric models (e.g., Jenkins et al., 2003).

Table 4c
Biomass ratios calculated based on site-specific information list in Table 2.

	MT	NR	MM	WC
C_{fr}:C_{lf}	0.75	–	1.21	1.34
C_{st}:C_{lf}	17.3	19.0	47.3	40.9
$C_{alloc,lf}$:C_{lf}[a]	0.18	0.28	0.93	0.80
$C_{alloc,wood}$:$C_{alloc,lf}$[b]	2.4	–	1.5	1.0

[a] An estimate of the parameter α_{lf}.
[b] An estimate of the parameter r_2.

The above discussions indicate that the original model parameters lead to an overestimated stem-to-leaf ratio, which could result in overestimation of vegetation (and soil) carbon stocks in Biome-BGC simulations (e.g., Pietsch and Hasenauer, 2006). Based on the theoretical analysis (Eq. (10d) in Appendix B), an effective way to decrease this ratio is to decrease carbon allocated to stem (the parameter r_2) or/and to increase tree's mortality (the total of β_{age} and β_{fire}, or β_{total}). On the other hand, site measurements indicate that the model parameter r_2 is reasonable for ENF and may be slightly overestimated for DBF (Table 4c). Therefore, we chose to tune down the stem-to-leaf ratio by increasing β_{total}, which is also the approach suggested by Pietsch and Hasenauer (2006). With the revised parameters (β_{total} of 0.025/year for both PFTs), the new estimated ratio is about 24 for ENF and 61 for DBF, more comparable (though not exactly the same) with the observations (Tables 4a–4c).

The adjustment of β_{total} can be explained in another way. It is clear that mortality mainly regulates the age structure of an ecosystem. For Biome-BGC, because it assumes that mortality happens uniformly to the simulated vegetation, it can be derived that the average age of the steady-state ecosystem is approximately the reciprocal of the total mortality ($1/\beta_{total}$). Therefore, the stand age of the simulated forests is around 40 years on average when β_{total} is 0.025 per year. Changes in β_{total} will induce changes in ages of the ecosystem as well as in the corresponding biomass ratios. In general, older forests have larger stem-to-leaf ratios than younger forests. For instance, if we change β_{total} of ENF to 0.05/year (i.e., average stand ages of 20 years) and 0.0125/year (i.e., average stand ages of 80 years), the stem-to-leaf ratio will be about 13 and 46, respectively. These results are in agreement with observations of a chronosequence of ponderosa pine stands at Metolius, where the corresponding ratio is about 9 for stands less than 20 years old, and is about 43 for stands older than 80 years (Law et al., 2003).

Because the biomass ratios depend only on the model parameters listed in Table 4a, they can be verified with model simulations even when the rest of the model is not fully calibrated. Fig. 4 shows time series of stem-to-leaf ratios simulated in model spin-up runs for all sites (the other biomass ratios are constant as listed in Table 4b and therefore not shown). For illustration, the spin-up runs were started with two different initial conditions with low/high stem-to-leaf ratios. However, as the simulations go on and become steady (which may take more than one thousand climate years), biomass ratios converge towards the theoretically estimated values in both cases (Fig. 4; Tables 4a–4c). The oscillatory variability of the time series at the beginning of the simulation (Fig. 4) is mainly induced by the spinup algorithms of Biome-BGC, which adds nitrogen to the system to speed up the growth of vegetation (Thornton and Rosenbloom, 2005).

From the biomass ratios in Tables 4a–4c we can estimate carbon stocks in all vegetation compartments (Table A1 of Appendix A) and important annual carbon fluxes of the simulated plants, including MR, GR, NPP, and more (Table 5). Here we focus on the

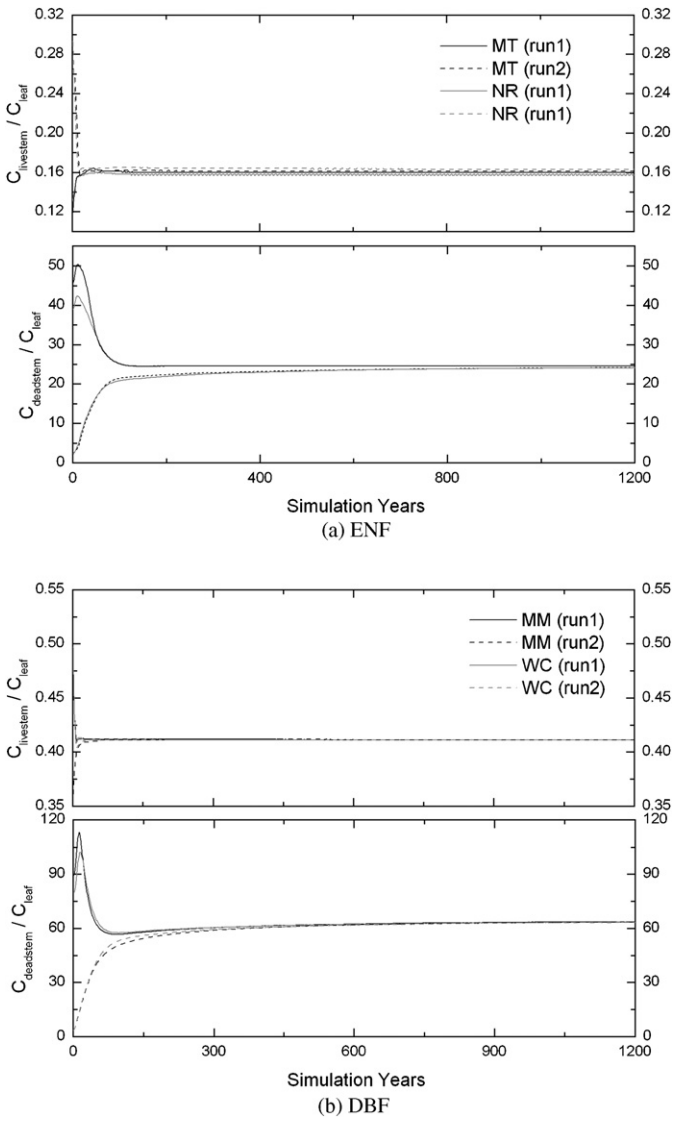

Fig. 4. Evolutions of biomass ratios in model "spin-up" simulations for (a) Evergreen Needle Forest and (b) Deciduous Broadleaf Forest. The two panels (from top to bottom) show biomass ratios between: (1) live stem and leaf; (2) dead stem and leaf, respectively. The notations of "run1" and "run2" indicate model experiments with different initial conditions.

two fluxes, $C_{pot,alloc}$ (carbon available for potential allocation) and $C_{act,alloc}$ (actually allocated carbon), for they help evaluate nitrogen limitation of the simulated ecosystem. For instance, at MT annual GPP is estimated at about 1.63 (kg C/m^2/year) and MR is about 0.48 (kg C/m^2/year); therefore, about 1.2 (kg C/m^2/year) of carbon is available for allocation ($C_{pot,alloc}$; Table 5). However, the independently estimated $C_{act,alloc}$ is only about 0.5 (kg C/m^2/year),

Table 5
Carbon fluxes (units: kg C/m^2/year) estimated in the second-tier model.

	MT	NR	MM	WC
GPP	1.63	1.14	1.48	1.61
MR	0.48	0.48	0.47	0.34
$C_{pot,alloc}$	1.15	0.66	1.01	1.27
$C_{act,alloc}$	0.49	0.52	0.84	0.95
GR	0.11	0.12	0.19	0.22
NPP[a]	0.38	0.40	0.65	0.73
$C_{act,alloc}/C_{pot,alloc}$	0.43	0.79	0.83	0.75

[a] Calculated as $C_{act,alloc}$ less GR.

Table 6
Nitrogen fluxes (units: g N/m^2/year) and f_{pi} estimated in the third-tier model.

	MT	NR	MM	WC
$N_{pot,alloc}$	12.8	7.9	17.9	23.9
$N_{act,alloc}$	4.9	5.2	13.1	14.4
$N_{retrans}$	1.7	1.8	4.6	5.1
N_{uptk}	3.2	3.4	8.5	9.2
f_{pi}	25%	43%	48%	38%
N_{min}	15.6	17.0	29.4	32.2
N_{immob}	12.8	13.9	21.1	23.1
$N_{loss,vol}$	0.16	0.17	0.30	0.33
$N_{loss,fire}$	0.34	0.29	0.29	0.38
N_{input}	0.50	0.46	0.59	0.71

approximately 43% of $C_{pot,alloc}$ (Table 5). Therefore, carbon allocation at MT (in the model) is considerably limited by nitrogen availability. Nitrogen limitation, although to less degrees, is also found at the other sites (Table 5).

Limited nitrogen availability is more formally quantified by the state variable f_{pi} (fraction of potential immobilization; Eq. (13) of Appendix B) in Biome-BGC. Based on the carbon budget of vegetation (Table 5) and the associated C:N ratios (Table A2), we estimate the corresponding nitrogen budget and f_{pi} for all sites (Table 6). At MT, the simulated vegetation would need about 12.8 (g N/m^2/yr) of nitrogen ($N_{pot,alloc}$) in order to allocate all its available carbon; however, the amount of nitrogen ($N_{act,alloc}$) it can actually get is about 4.9 (g N/m^2/yr), of which 1.7 (g N/m^2/yr) is from retranslocation ($N_{retrans}$) and about 3.2 (g N/m^2/yr) is uptake from the soil (N_{uptk}; Table 6). Therefore, f_{pi} (estimated as the ratio between N_{uptk} and $N_{pot,alloc}$) is about 25% (Table 6). The estimated f_{pi} ranges 38%–48% at the other sites (Table 6).

Once f_{pi} is known, we can estimate all carbon/nitrogen stocks and fluxes in the soil/litter pools. The estimated soil/litter carbon stocks are listed in Table A1 (Appendix A). The estimated nitrogen stocks, though not directly shown, can be inferred based on the carbon stocks (Table A1) and the C:N ratios (Table A2). Here we examine the estimated nitrogen fluxes for the rest of the ecosystem (Table 6). As shown, annually mineralized nitrogen is about 16 (g N/m^2/yr) at NR and MT, and about 30 (g N/m^2/yr) at MM and WC; the corresponding immobilized nitrogen is about 13 (g N/m^2/yr) and about 22 (g N/m^2/yr), respectively, accounting for 80% of mineralization at NR and MT, and 60% of mineralization at MM and WC. Most of the remaining mineralized nitrogen is taken up by the plants (Table 6), but a small proportion of nitrogen is released from the system, mainly through volatilization ($N_{loss,vol}$) and fire ($N_{loss,fire}$). The annual loss of nitrogen is about 0.5 (g N/m^2/yr) at MT and NR, and about 0.6–0.7 (g N/m^2/yr) at MM and WC (Table 6). The loss of nitrogen must be compensated by the input of nitrogen in to the system, which determines the overall rate of nitrogen deposition and fixation (N_{input}) at each site (Table 6).

The determination of N_{input} represents the last step in analyzing the second- and the third-tier model. With this information, as well as the parameters fine-tuned in the first-tier model, we then run the full BGC-Biome model to verify the calibrations and analyses discussed above. Fig. 5 shows the simulated ET, GPP, and LAI, along with the corresponding observations. As shown, the simulated LAI is consistent with that was prescribed in the first-tier model, which also dictates the agreement between the simulated ET and GPP fluxes and the observations (Fig. 5). Indeed, the final simulated ET and GPP are almost identical to those simulated by the calibrated first-tier model (not shown).

We also compare the simulated carbon stocks of the ecosystem with those previously estimated (Table A1 of Appendix A). Fig. 6 shows the scatter plots of the carbon stocks at all sites, with the abscissa (x-) and ordinate (y-) coordinates representing theoretical estimates and model simulations, respectively.

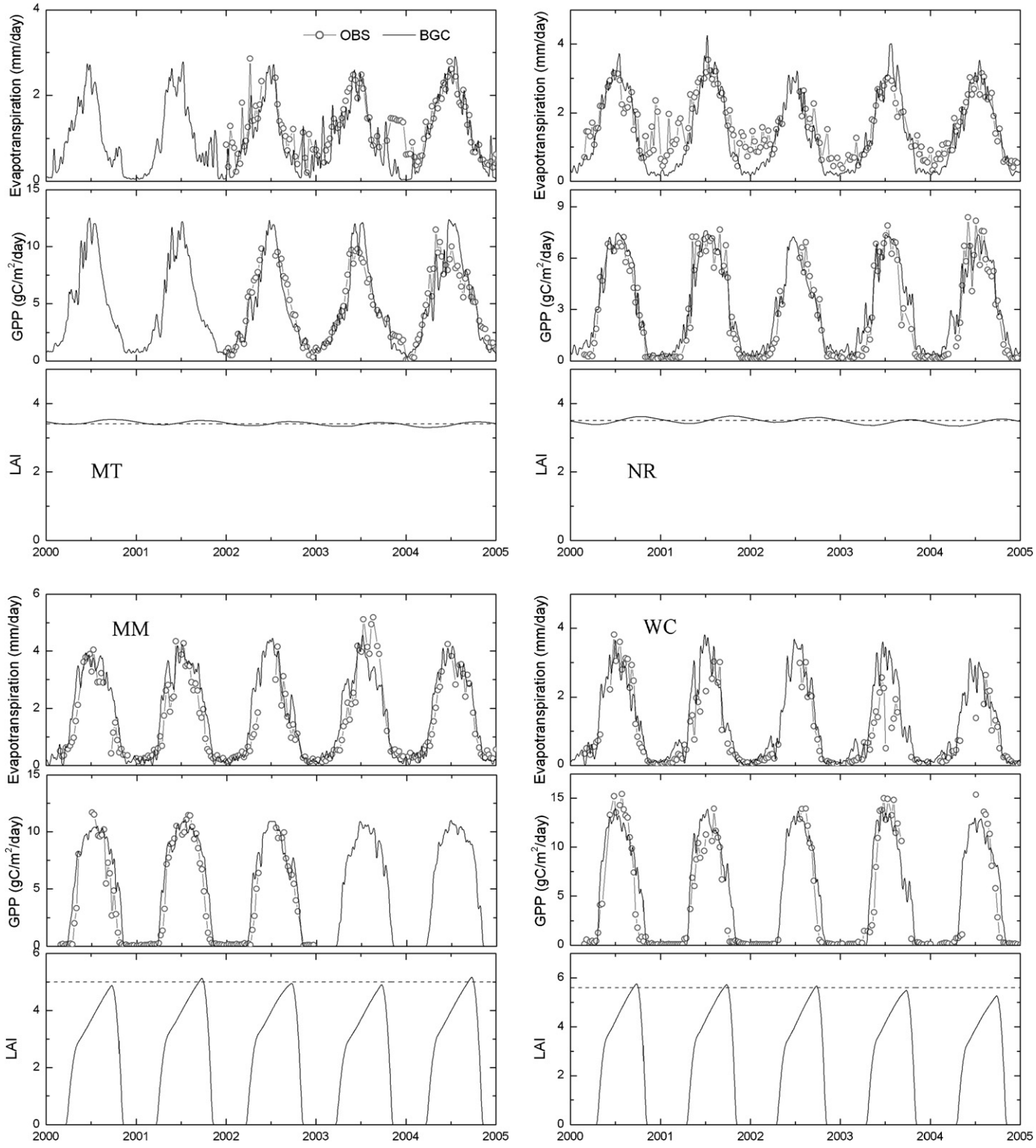

Fig. 5. ET, GPP, and LAI simulated by the calibrated Biome-BGC model (solid black lines; "BGC"), compared with the tower measurements (solid gray lines; "OBS").

There is good agreement between the two sets of results: all the plotted points, ranging from 0.01 (kg C/m^2, in living wood and fast-decaying soil pools) to 16 (kg C/m^2, in dead wood and slow-decaying soil pools), lie upon or adjacent to the 1-to-1 line (Fig. 6, upper panels). The only outliers are the two fast-decaying litter/soil pools (*litr*1 and *soil1*) at the two DBF sites, where the estimates are lower than simulations (Fig. 6). This is caused by the fact that these two carbon pools are small and are subject to relatively high seasonal variability (not shown), and thus the estimation of the annual mean carbon stocks is biased. However, this problem does not affect the estimation of the annual effluxes from these pools, which are constrained by the carbon balance relationship and thus by the influxes from the upstream carbon pools. Therefore, estimation errors of the two compartments do not propagate to the estimates of other soil/litter pools (Fig. 6).

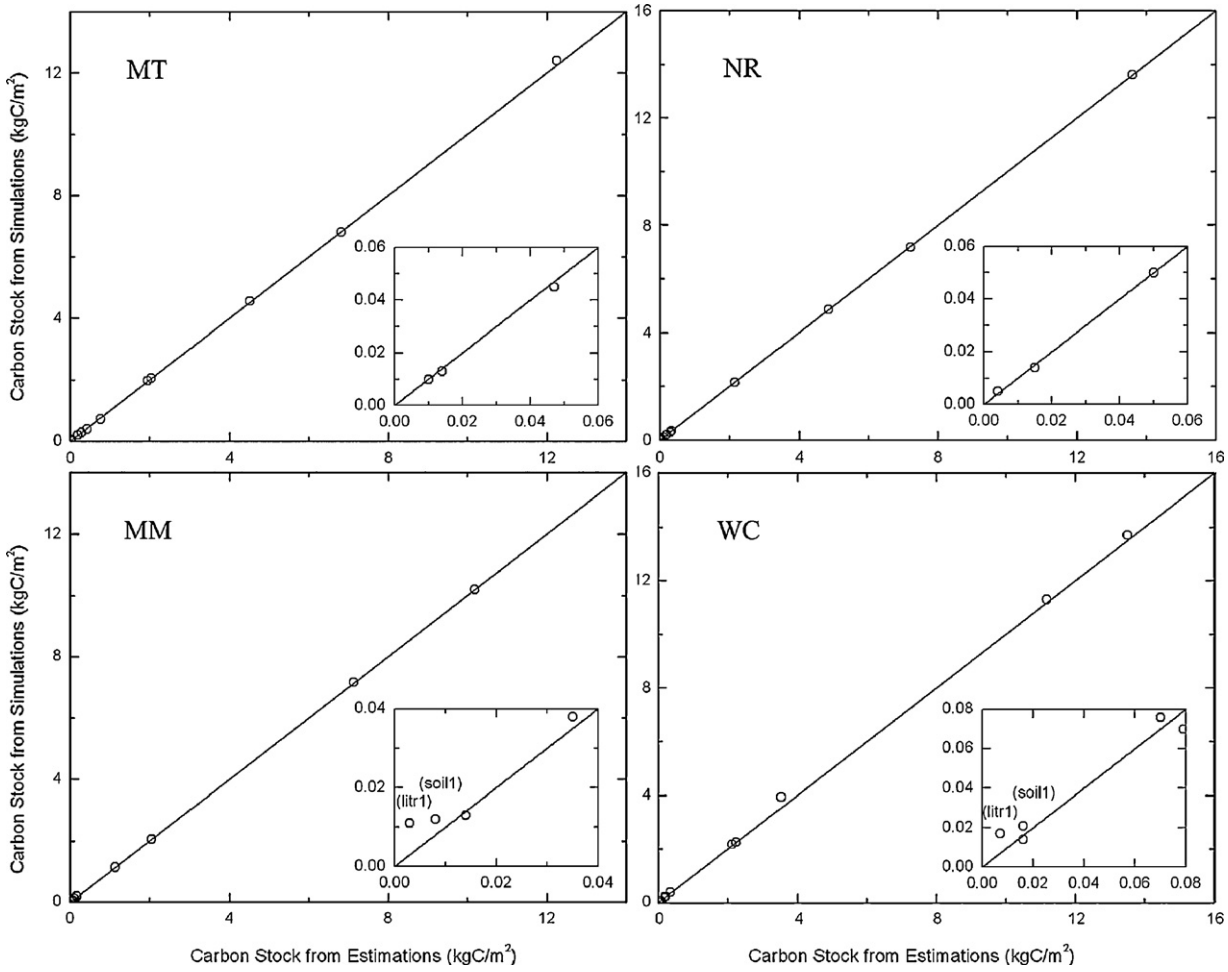

Fig. 6. Comparison between carbon stocks estimated by the hierarchical analysis (of the second- and the third-tier models) and simulated by the calibrated Biome-BGC model.

3.3. Discussion

Above we demonstrated how to apply the proposed model hierarchy to tune a few selected parameters of Biome-BGC so that the model can closely simulate observed ET, GPP, LAI, and some other ecological attributes (e.g., aboveground biomass). Because of the optimization techniques involved, this process is sometimes called "parameter optimization", and the obtained parameters are called "optimal parameters" (e.g., Jackson et al., 2003; Mo et al., 2008). However, the word "optimization" here may not be interpreted in a physiologically meaningful way. For instance, in the first-tier model the fine-tuned maximum stomatal conductance ($g_{s,max}$) at the two DBF sites is about half of its original values (0.0025 m/s versus 0.0050 m/s; Table 3): the new $g_{s,max}$ renders better simulation results, but it is discernibly lower than values commonly reported in the literature (e.g., Larcher, 2003). Although this discrepancy can be explained by the fact that there are considerable site-to-site variations in $g_{s,max}$ (Kelliher et al., 1995) and thus the adjusted values are still valid, it may also suggest other issues in the model that are not covered by the current analysis. Indeed, it is found that when LAI is high (3 or greater), light-use efficiency in the current Biome-BGC may be too high (unpublished results).

The hierarchical analysis scheme allows us to diagnose some other aspects of the model. In the second-tier model, for instance, the modeled maintenance respiration (MR) and growth respiration (GR) is usually not sufficient to explain the difference between GPP and NPP (Table 5), and an additional pathway must be introduced to help remove the surplus carbon when necessary (see Appendix B for details). Reasons for this discrepancy remain unknown: it may indicate that our knowledge of respiration is still very limited, or alternatively, it suggests that NPP is underestimated. In the latter case, because the simulated aboveground NPP is calibrated based on observations, it also suggests that a portion of NPP may not be captured by the current measurements. Furthermore, in current Biome-BGC insufficient allocation is always attributed to restricted nitrogen availability. Although it is probably true because temperate forests are generally nitrogen limited (Magnani et al., 2007), the extent to which nitrogen is limiting vegetation growth in the model is however questionable for that as discussed above, any bias in simulated respiration can lead to incorrect nitrogen budget. Limited by the used dataset, this study does not examine the soil nitrogen budget of Biome-BGC with observations. We recognize this limitation, and expect to address it in the future.

Finally, it needs to be pointed out that the analysis of the second- and the third-tier model in this study is solely based on the equilibrium assumption, while such equilibrium can hardly be observed at individual flux-tower sites (including the four sites in this study). Indeed, site studies indicate that old-growth forests (with ages of hundreds of years) may still accumulate carbon (Luyssaert et al., 2008). One reason for this mismatch may be the fact that the sequestration of atmospheric carbon is a "slow-in, rapid-out" process, and the "rapid-out" carbon fluxes (released by disturbances such as fire) are difficult to monitor by flux towers (Körner, 2003). On the other hand, vegetation simulated by Biome-BGC (or other similar ecosystem models) inherently accounts for disturbances like fire and mortality of various causes, and it thus represents

a statistical average of forests of different ages (as discussed earlier in the paper). For this reason, in calibrating the second-tier model we compared the derived biomass ratios not only to site measurements, but also to allometric models (Jenkins et al., 2003), in order to make the analysis more general. Nevertheless, we recognize that the equilibrium analysis approach alone is insufficient for non-steady ecosystems (e.g., forests that have undergone recent major disturbances or partial disturbances such as ground fire or thinning). In this case, the dynamic characteristics of the model around the equilibrium must be taken into account (Thornton et al., 2002). Dynamical analysis of ecosystem models can also be conducted under the proposed hierarchical model scheme, which we expect to address in future studies.

4. Conclusions

This study develops a hierarchical scheme to analyze and calibrate the terrestrial ecosystem model Biome-BGC. Under this scheme, Biome-BGC is divided into three functionally cascaded tiers. The first-tier model focuses on ecophysiological processes at the leaf level. It allows LAI in the model to be specified based on *a priori* information (usually observations), and simulates observed evapotranspiration and photosynthesis with the prescribed LAI. The restriction on prescribed LAI is then lifted in the following two tiers, which analyze how carbon and nitrogen is cycled in the simulated ecosystem to dynamically support the prescribed canopy. In particular, the second-tier model considers the cycling of carbon at the whole-plant level. Based on the principle of carbon balance, it estimates biomass storage in all vegetation components and their demands for annual carbon allocation directly from the prescribed (and thus observed) LAI and the allometric allocation relationships described in Biome-BGC. By comparing carbon that is potentially available for allocation with carbon that is actually allocated, this tier of the model also evaluates how vegetation carbon allocation is limited by soil nitrogen availability. The third-tier model extends the methodology of the second tier to analyze carbon/nitrogen stocks and fluxes in all litter/soil pools. It calculates nitrogen fluxes of mineralization and immobilization resulting from the decomposition of soil organic matter and litter biomass. It also estimates nitrogen fluxes that are escaped from the ecosystem during these processes, and finally, determines how much nitrogen must be input annually to meet the total nitrogen balance of the simulated ecosystem.

This model hierarchy is examined with model experiments at four AmeriFlux sites. The results indicate that this approach simplifies the calibration of Biome-BGC, and also helps to diagnose the internal status of the model, which is difficult by conventional calibration algorithms. In addition, the results indicate good agreement between carbon/nitrogen stocks estimated by the derived methods and those by model simulations, suggesting they may find applications in solving the problem of model spin-up, especially for applications over large regions. However, because these methods are derived based on the assumption of equilibrium, they cannot directly be applied to analyze non-steady ecosystems. Future efforts are needed to analyze the dynamic characteristics of the model under the proposed hierarchical scheme.

Finally, although this paper mainly focuses on analyzing Biome-BGC, the general concept and methodology developed in this study may help analyze other similar ecosystem models as well.

Acknowledgements

This research was supported by funding from NASA's Science Mission Directorate through EOS. The views expressed herein are those of the authors and do not necessarily reflect the views of NASA. Flux tower measurements were funded by the Department of Energy, the National Oceanic and Atmospheric Administration, the National Space Agency (NASA) and the National Science Foundation. The Metolius research was supported by the Office of Science (BER), U.S. Department of Energy (DOE, Grant no. DE-FG02-06ER64318). Special thanks to Drs. Russell Monson, Danilo Dragoni, and Kenneth Davis for providing flux data at Niwot Ridge, Morgan Monroe State Forest, and Willow Creak. Research at the MMSF is supported by the Office of Science (BER), US-DOE, Grant No. DE-FG02-07ER64371. The authors are grateful to two anonymous reviewers for their constructive comments and suggestions. We also thank Dr. Jennifer Dungan for helpful feedback on an earlier version of this manuscript. W. Wang thanks Dr. Masao Kanamitsu for initial discussions on the Held (2005) paper.

Appendix A. Supplemental tables

Table A1
Estimated carbon stocks in ecosystem compartments (Unit: kg C/m^2).

	MT	NR	MM	WC
lf	0.28	0.30	0.17	0.19
fr	0.28	0.30	0.17	0.19
lst	0.047	0.050	0.071	0.079
dst	6.81	7.21	10.18	11.18
lcr	0.014	0.015	0.014	0.016
dcr	2.04	2.16	2.04	2.24
cwd	4.51	4.84	2.05	3.54
*litr*1	0.010	0.004	0.003	0.007
*litr*2	0.42	0.18	0.09	0.19
*litr*3	0.20	0.09	0.04	0.07
*litr*4	0.76	0.34	0.16	0.35
*soil*1	0.010	0.011	0.008	0.016
*soil*2	0.19	0.21	0.11	0.22
*soil*3	1.95	2.16	1.13	2.14
*soil*4	12.25	13.61	7.12	13.51

Table A2
C:N ratios of ecosystem compartments (Unit: kg C/kg N)[a].

	ENF (MT, NR)	DBF (MM, WC)
$C{:}N_{lf}$	42	24
$C{:}N_{lf,dead}$	93	49
$C{:}N_{fr}$	42	42
$C{:}N_{lst}$, $C{:}N_{lcr}$	50	50
$C{:}N_{dst}$, $C{:}N_{dcr}$	729	442
$C{:}N_{cwd}$	721	437
$C{:}N_{litr1}$	59	46
$C{:}N_{litr2}$	153	75
$C{:}N_{litr3}$	56	42
$C{:}N_{litr4}$	114	65
$C{:}N_{soil1}$	12	12
$C{:}N_{soil2}$	12	12
$C{:}N_{soil3}$	10	10
$C{:}N_{soil4}$	10	10

[a] C:N ratios of vegetation and soil pools are prescribed model parameters, while C:N ratios of litter and CWD pools are not prescribed but estimated using algorithms discussed in the text.

Appendix B. Derivation of the model hierarchy

This appendix discusses in detail how to analyze and calibrate the proposed model hierarchy of Biome-BGC. It identifies the parameters for calibration of ET and GPP in the first-tier model and derives mass-balance equations to estimate carbon/nitrogen fluxes in the second-tier and the third-tier models. Yet it is impossible to cover all components of Biome-BGC in this paper. For more detailed discussions of Biome-BGC, we refer the reader to Thornton (1998) and Thornton et al. (2002).

B.1. First-tier model

The first-tier model simulates ET and GPP with prescribed LAI. To calibrate the model, we consider the water-cycle component first.

Biome-BGC simulates water fluxes evaporated from the soil surface and vegetation canopy (i.e., intercepted precipitation), transpired by vegetation, and sublimated from the snowpack. Of these fluxes, sublimation of snow and evaporation of intercepted water occur under certain conditions (i.e., when there is snow on the ground and on rainy days, respectively), which can be relatively easily differentiated in observations. In addition, for well-vegetated sites, evaporation from the soil surface is generally less important than transpiration from canopy. Therefore, the main focus here is how to calibrate the transpiration of soil water by vegetation.

Biome-BGC uses the Penman–Monteith equation to estimate evapotranspiration rate (ET, per projected leaf area), which can also be represented as a diffusive process (Sellers et al., 1997):

$$\mathrm{ET} = g_\mathrm{v}[e^*(T_\mathrm{s}) - e_\mathrm{a}]\frac{\rho c_p}{\lambda\gamma}, \tag{1}$$

where g_v is the leaf-level conductance for water vapor, $e^*(T_\mathrm{s})$ is the saturation water vapor pressure at leaf temperature T_s, e_a is the water vapor pressure of the ambient air; ρ, c_p, λ, and γ represent the density and specific heat of air, the latent heat of evaporation, and the psychrometric constant.

In Eq. (1), leaf water conductance (g_v) is mainly regulated by stomatal conductance (g_s), which is modeled as a product of a maximum value ($g_{\mathrm{s,max}}$) and a series of multiplicative regulators (valued between 0 and 1) that respond to incident radiation (R), vapor pressure deficit (VPD), minimum temperature (T_min), and soil water potential (Ψ), that is,

$$g_\mathrm{s} = m(R)\cdot m(\mathrm{VPD})\cdot m(T_\mathrm{min})\cdot m(\Psi)\cdot g_{\mathrm{s,max}} \tag{2}$$

where m represents the regulator functions. Approximate g_v with g_s by substituting Eq. (2) into Eq. (1), giving

$$\mathrm{ET} = m(R)m(\mathrm{VPD})m(T_\mathrm{min})m(\Psi)g_{\mathrm{s,max}}[e^*(T_\mathrm{s}) - e_\mathrm{a}]\frac{\rho c_p}{\lambda\gamma}. \tag{3}$$

In Eq. (3), ρ, c_p, λ, and γ are physical constants; VPD and T_min are climate variables that are externally determined; and the incident radiation, R, and the vapor pressure difference, $e^*(T_\mathrm{s}) - e_\mathrm{a}$, are also mainly determined by climate variables. Therefore, an effective way to calibrate ET is to adjust the maximum stomatal conductance, $g_{\mathrm{s,max}}$, and another parameter that affects soil water potential (Ψ). For the latter, because variations of Ψ strongly depend on soil water-holding capacity, we choose the effective depth of soil (d_eff, also known as the rooting depth) as the second parameter to tune.

Next, we consider the photosynthesis component. Biome-BGC estimates the carbon assimilation rate (A, per projected leaf area) by constraining the Farquhar model (Farquhar et al., 1980) with a CO_2 diffusion equation,

$$A = g_\mathrm{c}(C_\mathrm{a} - C_\mathrm{i}), \tag{4}$$

where C_a and C_i represent atmospheric and intracellular CO_2 concentration, respectively; g_c is the leaf-level conductance for CO_2, which is related to the conductance of water (g_v) by

$$g_\mathrm{c} = \frac{g_\mathrm{v}}{1.6}. \tag{5}$$

Therefore, photosynthesis is closely related to transpiration, and once g_v is determined, g_c is determined as well.

In Biome-BGC, Eq. (4) is substituted into the Farquhar model to eliminate the unknown variable C_i, so that the assimilation rate A can be solved. For brevity, the Farquhar model is not presented here (but see Farquhar et al., 1980 for detailed discussion). It is sufficient to indicate that A mainly depends on leaf temperature and leaf nitrogen, which influence the specific activity and the amount of the Rubisco enzyme, respectively (Thornton et al., 2002). Because temperature is a climate variable, we consider how to adjust leaf nitrogen, which is determined by specific leaf area (SLA), the leaf C:N ratio ($\mathrm{C{:}N_{leaf}}$), and the fraction of leaf nitrogen in the Rubisco enzyme (f_lnr). Of these variables, f_lnr has the smallest effect on the rest of carbon/nitrogen cycle (see below), and thus it is chosen as the third parameter to calibrate the rate of photosynthesis.

B.2. Second-tier model

In the second-tier model, we focus on analyzing the plant-level carbon/nitrogen cycles at system equilibrium. First, we consider the question of how much carbon is required to support leaf growth, given the assumption that maximum LAI (for DBF) or mean LAI (for ENF) does change year to year. (For simplicity, below we use maximum LAI as the example to derive the equations. For evergreen forests, LAI simulated by Biome-BGC is almost constant, and thus annual maximum LAI closely approximates as annual mean LAI). Based on the principle of mass balance, carbon allocated to leaves must be balanced by carbon lost via litterfall and mortality, that is,

$$C_\mathrm{l,alloc} = (1 + f_\mathrm{gr})\cdot(\alpha + \beta)\cdot C_\mathrm{l,max}, \tag{6}$$

where $C_\mathrm{l,alloc}$ indicates newly allocated leaf carbon; $C_\mathrm{l,max}$ denotes leaf carbon corresponding to maximum LAI; α and β represent the annual rates of litterfall and overall mortality (the total of β_age and β_fire shown in Tables 1a–1c), respectively; and f_gr indicates the fraction of carbon that is respired during the growth process, which is assumed to be 0.3 in Biome-BGC. Note that Eq. (6) was derived for evergreen forests based on the assumption that leaf carbon is always $C_\mathrm{l,max}$. For deciduous forests, because trees shed all their leaves every year, the annual total loss of leaf carbon is approximately $C_\mathrm{l,max}$, that is, the sum of α and β is 1.

Eq. (6) indicates that $C_\mathrm{l,alloc}$ can be estimated based on $C_\mathrm{l,max}$. At the same time, according to the allometric allocation scheme assumed in Biome-BGC, carbon allocated to other vegetation compartments is directly or indirectly proportional to $C_\mathrm{l,alloc}$. For woody species, these compartments include fine root, live/dead stem, and live/dead coarse root, and the corresponding carbon fluxes are:

$$C_\mathrm{fr,alloc} = r_1\cdot C_\mathrm{l,alloc} \quad \text{(fine roots)} \tag{7a}$$

$$C_\mathrm{lst,alloc} = r_2\cdot r_3\cdot C_\mathrm{l,alloc} \quad \text{(live stem)} \tag{7b}$$

$$C_\mathrm{dst,alloc} = r_2\cdot(1 - r_3)\cdot C_\mathrm{l,alloc} \quad \text{(dead stem)} \tag{7c}$$

$$C_\mathrm{lcr,alloc} = r_4\cdot r_2\cdot r_3\cdot C_\mathrm{l,alloc} \quad \text{(live coarse root)} \tag{7d}$$

$$C_\mathrm{dcr,alloc} = r_4\cdot r_2\cdot(1 - r_3)\cdot C_\mathrm{l,alloc} \quad \text{(dead coarse root)} \tag{7e}$$

where rs denote allometric parameters (Tables 1a–1c). Together, the total amount of annually allocated carbon is estimated as:

$$C_\mathrm{act,alloc} = (1 + r_1 + r_2 + r_2 r_4)\cdot C_\mathrm{l,alloc}. \tag{8}$$

and the annual growth respiration (GR) is:

$$\mathrm{GR} = \frac{f_\mathrm{gr}}{1 + f_\mathrm{gr}}\cdot C_\mathrm{act,alloc} \approx 0.23\cdot C_\mathrm{act,alloc}, \tag{9}$$

where a constant value of 0.3 is assumed for the parameter f_gr.

As in Eq. (6), we can write carbon balance equations for all the plant compartments described above. Because the newly allocated carbon to these compartments is already known (Eq. (7)), these balance relationships can be inverted to estimate their carbon stocks in term of $C_\mathrm{l,max}$. For live tissues (i.e., fine roots, live stem/coarse root), because they go through similar aging processes (e.g., litterfall or turnover) as leaves, the following relationships can be formulated:

$$C_\mathrm{fr,max} = \frac{\alpha_l + \beta}{\alpha_{fr} + \beta}\cdot r_1\cdot C_\mathrm{l,max} \quad \text{(fine roots)} \tag{10a}$$

$$C_{lst} = \frac{\alpha_l + \beta}{\alpha_{lst} + \beta} \cdot r_2 \cdot r_3 \cdot C_{l,max} \quad \text{(live stem)} \tag{10b}$$

$$C_{lcr} = \frac{\alpha_l + \beta}{\alpha_{lcr} + \beta} \cdot r_4 \cdot r_2 \cdot r_3 \cdot C_{l,max} \quad \text{(live coarse root)} \tag{10c}$$

where αs represent the rate of litterfall/turnover of the corresponding tissues. For dead woody tissues (i.e., dead stem/coarse root), they gain carbon from the turnover process of their live counterparts, and they lose carbon only when the whole plant dies. The equations to estimate their biomass are thus:

$$C_{dst} = \left[\frac{\alpha_l + \beta}{\beta} \cdot r_2 \cdot (1 - r_3) + \frac{\alpha_{lst}}{\beta} \cdot \frac{\alpha_l + \beta}{\alpha_{lst} + \beta} \cdot r_2 \cdot r_3 \right] \cdot C_{l,max}$$

(dead stem) (10d)

$$C_{dcr} = \left[\frac{\alpha_l + \beta}{\beta} \cdot r_4 \cdot r_2 \cdot (1 - r_3) + \frac{\alpha_{lcr}}{\beta} \cdot \frac{\alpha_l + \beta}{\alpha_{lcr} + \beta} \cdot r_4 \cdot r_2 \cdot r_3 \right] \cdot C_{l,max}$$

(dead coarse root) (10e)

In Biome-BGC, the default litterfall rate of fine roots (α_{fr}) is the same as leaves (α_l), and the turnover rate of live stem (α_{lst}) is the same as live coarse root (α_{lcr}). It thus can be derived from Eq. (10) that:

$$C_{fr,max} = r_1 \cdot C_{l,max} \quad \text{(fine roots)} \tag{10a'}$$

$$C_{lcr} = r_4 \cdot C_{lst} \quad \text{(live coarse root)} \tag{10c'}$$

$$C_{dcr} = r_4 \cdot C_{dst} \quad \text{(dead coarse root)} \tag{10e'}$$

Eq. (10) allows us to estimate carbon stocks for all vegetation compartments. From the corresponding C:N ratios prescribed in Biome-BGC, their nitrogen content is also determined. On this basis, we can further calculate the annual maintenance respiration (MR) for these components by (Thornton, 1998):

$$MR = 0.218 \cdot N \cdot Q_{10}^{(T-20)/10} \tag{11}$$

where N and T indicate the nitrogen content and the temperature of the component, respectively; the Q_{10} factor is assumed to be 2.0 for all components.

Based on the estimated annual GPP (from the first-tier model) and MR (Eq. (11)), the amount of carbon that is potentially available for allocation ($C_{pot,alloc}$) can be estimated as,

$$C_{pot,alloc} = GPP - MR \tag{12}$$

On the other hand, the actually allocated carbon, $C_{act,alloc}$, is given by Eq. (8). Per Biome-BGC algorithms, $C_{act,alloc}$ is the same as $C_{pot,alloc}$ only if vegetation growth is not restrained by available nutrients (i.e., mineral nitrogen); otherwise the surplus carbon ($C_{pot,alloc} - C_{act,alloc}$) is removed from the system[1]. The difference between $C_{pot,alloc}$ and $C_{act,alloc}$ thus provides a measure by which to evaluate whether/how the simulated vegetation growth is limited by nitrogen availability. This subject will be further discussed in the next section.

B.3. Third-tier model

The decomposition of litter and soil organic matter is generally limited by soil mineral nitrogen. Per Biome-BGC algorithms, the two main demands for mineral nitrogen are plant uptake and soil immobilization. When soil mineral nitrogen (N_{smin}) cannot meet the total demands from the two components, the actual allocations (i.e., $N_{act,uptk}$ and $N_{,act,immb}$) are made proportionally to their potential demands (i.e., $N_{pot,uptk}$ and $N_{pot,immb}$). Therefore, when N_{smin} is limited, the following ratios are the same:

$$f_{pi} = \frac{N_{act,immb}}{N_{pot,immb}} = \frac{N_{act,uptk}}{N_{pot,uptk}} = \frac{N_{s,min}}{N_{pot,immb} + N_{pot,uptk}}, \tag{13}$$

where f_{pi} stands for "the fraction of potential immobilization", a state variable defined in Biome-BGC.

Eq. (13) indicates that f_{pi} can be estimated from nitrogen uptake by vegetation. Indeed, $N_{pot,uptk}$ is directly estimated from $C_{pot,alloc}$ (Eq. (12)) based on the C:N ratios of different vegetation compartments. Similarly, the nitrogen actually allocated ($N_{act,alloc}$) can be estimated from $C_{act,alloc}$ (Eq. (8)). Finally, to estimate $N_{act,uptk}$ from $N_{act,alloc}$ we need to deduct the portion of nitrogen (N_{trans}) that is retranslocated within the plant[2]. Based on the carbon/nitrogen stocks in different vegetation compartments (estimated in the second-tier model) and their decay rate, the calculation of N_{trans} is straightforward and therefore neglected here.

Once f_{pi} is known, we are ready to estimate carbon/nitrogen stocks in all the four litter pools (and a coarse woody debris pool) and the four soil pools defined in Biome-BGC. These pools are linked in a manner that carbon and nitrogen always flow from faster-decaying pools to slower decaying pools, and thus the inflow of a pool is determined solely by the outflow of its upstream pools (a detailed diagram can be found in Thornton and Rosenbloom, 2005). Because the most-upstream pools (i.e., plant compartments) are all known, carbon/nitrogen stocks in these soil/litter pools, as well as the fluxes among them, can be sequentially estimated.

To illustrate, we consider the case of the labile litter pool, which is the first litter pool in Biome-BGC. This pool contains the labile portion of the leaf and fine root litter, and a part of newly allocated carbon/nitrogen that enters the pool when the whole plant dies. Therefore, the total inflow to the labile litter pools is:

$$X_{litr1}^{inflow} = p_{lab} \cdot [(\alpha_l + \beta_{age}) \cdot X_{l,max} + (\alpha_{fr} + \beta_{age}) \cdot X_{fr,max}] + \beta_{age} \cdot 0.5 \cdot X_{act,alloc} \tag{14}$$

where X denotes either "C" (carbon) or "N" (nitrogen) and p_{lab} is a model parameter that represents the labile proportion of leaf and fine root litter. The constant factor (0.5) in the last term of Eq. (14) represents the proportion of allocated carbon and nitrogen that is stored for vegetation growth in the next growing season (Thornton, 1998). Note that all variables in Eq. (14) are known.

The outflow of the labile pool is induced by fire and by decomposition, that is,

$$X_{litr1}^{outflow} = (\beta_{fire} + f_{pi} \cdot m_{corr} \cdot k_{litr1}) \cdot X_{litr1} \tag{15}$$

where β_{fire} indicates fire-induced mortality; k_{litr1} is the base decomposition rate of this litter pool (specified by model parameters), while m_{corr} represents the regulation of climate variations on the decomposition rate. The calculation of m_{corr} mainly involves soil temperature and soil moisture, which are determined based on the results of the first-tier model.

At system equilibrium, the inflow of carbon and nitrogen in Eq. (14) must be balanced by the outflow in Eq. (15). Therefore, the only unknown variable in Eq. (15), X_{litr1}, is determined. Subsequently, the components of the outflow [on the right-hand-side of Eq. (15)] can be calculated, which then are used to estimate the heterotrophic respiration (HR), fire emissions (of carbon and nitrogen), and the

[1] In the original Biome-BGC, the surplus carbon is removed by reducing GPP by the corresponding amount; in this study, however, we revised the model to remove the surplus carbon by increasing the total amount of autotrophic respiration.

[2] In Biome-BGC, N_{trans} is calculated for turnover leaf and wood (stem and coarse root) by the N difference between living leaf/wood and dead leaf/wood, which have different C:N ratios.

carbon/nitrogen inflow for the next downstream pool (in this case, it is the fast microbial recycling pool in soil):

In the example above, the mass balance relationship is used twice to estimate the carbon and the nitrogen stocks of the labile litter pool separately. This is because in Biome-BGC the C:N ratios of the litter pools are not fixed but dynamically simulated. For the soil pools, on the other hand, their C:N ratios are prescribed by model parameters. In this case, carbon fluxes and stocks should be estimated first, and then converted to their nitrogen counterparts based on corresponding C:N ratios. It should be noted that the nitrogen inflow estimated based on the carbon inflow may not be the same as that estimated from the outflows from the upstream pools (as in Eq. (14)). When the latter is higher than the former, extra nitrogen is diverted into a special soil nitrogen pool (i.e., mineralization); in the opposite situation, nitrogen is taken from the soil nitrogen pool to cover the deficit (i.e., immobilization).

Through processes of mineralization, immobilization, and uptake (by vegetation), most nitrogen that enters into soil/litter pools is recycled within the ecosystem. There are only a few nitrogen fluxes that ultimately escape from the system. For Biome-BGC, the most important nitrogen effluxes include fire emission (as suggested by Eq. (15)) and nitrogen volatilization, which occurs in the process of mineralization and is proportional to the mineralized nitrogen. Because soil mineral nitrogen is usually in deficit (in the model), nitrogen leaching is generally less important than the two effluxes mentioned above.

To keep the nitrogen balance of the whole ecosystem, the above nitrogen effluxes must be compensated by influxes of nitrogen that enter the system. In Biome-BGC, these nitrogen influxes include nitrogen deposition and fixation, both of which are specified by model parameters. To close the nitrogen budget, therefore, a simple way is to adjust the rates of nitrogen deposition and fixation so that they are the same as the total effluxes. Alternatively, we can also adjust the size of the nitrogen/carbon pools (or their C:N ratios) so that the resulted effluxes match with the influxes—this can be done following the scheme outlined in the above sections, and thus is not elaborated.

Finally, it should be noted that for the carbon cycle, all effluxes (respiration and fire emissions) are derived from the primary carbon influx, GPP, following the principle of mass balance. Therefore, the carbon balance of the whole ecosystem is automatically ensured.

References

Cairns, M.A., Brown, S., Helmer, E.H., Baumgardner, G.A., 1997. Root biomass allocation in the world's upland forests. Oecologia 111, 1–11.

Campbell, G.S., Norman, J.M., 1998. An introduction to environmental biophysics. Springer-Verlag, pp. 286.

Cook, B.D., Davis, K.J., Wang, W., Desai, A.R., Berger, B.W., et al., 2004. Carbon exchange and venting anomalies in an upland deciduous forest in northern Wisconsin, USA. Agricultural and Forest Meteorology 126, 271–295.

Cramer, W., Kicklighter, D.W., Bondeau, A., Moore III, B., Churkina, G., et al., 1999. Comparing global models of terrestrial net primary productivity (NPP): overview and key results. Global Change Biology 5, 1–15.

Curtis, P.S., Hanson, P.J., Bolstad, P., Barford, C., Randolph, J.C., Schmid, H.P., Wilson, K.B., 2002. Biometric and eddy-covariance based estimates of annual carbon storage in five eastern North American deciduous forests. Agricultural and Forest Meteorology 113, 3–19.

Falge, E., Baldocchi, D., Olsonb, R., Anthonic, P., Aubinetd, M., et al., 2001. Gap filling strategies for long term energy flux data sets. Agricultural and Forest Meteorology 107, 71–77.

Farquhar, G.D., von Caemmerer, S., Berry, J.A., 1980. A biochemical model of photosynthetic CO_2 assimilation in leaves of C3 species. Planta 149, 78–90.

Harmon, R., Challenor, P., 1997. A Markov chain Monte Carlo method for estimation and assimilation into models. Ecological Modelling 101, 41–59.

Held, I.M., 2005. The gap between simulation and understanding in climate modeling. Bulletin of American Meteorological Society 86, 1609–1614.

IPCC, 2007. Climate Change 2007: The Physical Science Basis: Contribution of Working Group I to the Fourth Assessment Report of the Intergovernmental Panel on Climate Change [Solomon, S., D. Qin, M. Manning, Z. Chen, M. Marquis, K.B. Averyt, M. Tignor and H.L. Miller (eds.)]. Cambridge University Press, 996 pp.

Jackson, C., Xia, Y., Sen, M.K., Stoffa, P.L., 2003. Optimal parameter and uncertainty estimation of a land surface model: a case study using data from Cabauw, Netherlands. Journal of Geophysical Research 108, doi:10.1029/2002JD002991.

Jenkins, J.C., Chojnacky, D.C., Heath, L.S., Birdsey, R.A., 2003. National-scale biomass estimators for United States Tree Species. Forest Science 49, 12–35.

Jolly, W.M., Graham, J.M., Michaelis, A., Nemani, R.R., Running, S.W., 2005. A flexible, integrated system for generating meteorological surfaces derived from point sources across multiple geographic scales. Environmental Modeling and Software 20, 873–882.

Kelliher, F.M., Leuning, R., Raupach, M.R., Schulze, E.-D., 1995. Maximum conductances for evaporation from global vegetation types. Agricultural and Forest Meteorology 73, 1–16.

Knorr, W., Kattge, J., 2005. Inversion of terrestrial ecosystem model parameter values against eddy covariance measurements by Monte Carlo sampling. Global Change Biology 11, 1333–1351.

Körner, C., 2003. Slow in, rapid out—carbon flux studies and Kyoto targets. Science 300, 1242–1243.

Larcher, W., 2003. Physiological Plant Ecology, fourth ed. Springer, 513 pp.

Law, B.E., Sun, O.J., Campbell, J., van Tuyl, S., Thornton, P.E., 2003. Changes in carbon storage and fluxes in a chronosequence of ponderosa pine. Global Change Biology 9, 510–524.

Law, B.E., Turner, D., Campbell, J., Sun, O.J., Van Tuyl, S., Ritts, W.D., Cohen, W.B., 2004. Disturbance and climate effects on carbon stocks and fluxes across western Oregon USA. Global Change Biology 10, 1429–1444.

Law, B.E., T. Arkebauer, J.L. Campbell, J. Chen, O. Sun, M. Schwartz, C. van Ingen, S. Verma, 2009. Terrestrial Carbon Observations: Protocols for Vegetation Sampling and Data Submission. Report 55, Global Terrestrial Observing System. FAO, Rome. 87 pp.

Luyssaert, S., Schulze, E.-D., Börner, A., Knohl, A., Hessenmöller, D., Law, B.E., Ciais, P., Grace, J., 2008. Old-growth forests as global carbon sinks. Nature 455, 213–215.

Magnani, F., Mencuccini, M., Borghetti, M., Berbigier, P., Berninger, F., et al., 2007. The human footprint in the carbon cycle of temperate and boreal forests. Nature 447, 848–850.

Martin, J.G., Bolstad, P.V., 2005. Annual soil respiration in broadleaf forests of northern Wisconsin: influence of moisture and site biological, chemical, and physical characteristics. Biogeochemistry 73, 149–182.

Masson, V., Champeaux, J.-L., Chauvin, F., Meriguet, C., Lacaze, R., 2003. A global database of land surface parameters at 1-km resolution in meteorological and climate models. Journal of Climate 16, 1261–1282.

McGuire, A.D., Melillo, J.M., Joyce, L.A., Kicklighter, D.W., Grace, A.L., et al., 1992. Interactions between carbon and nitrogen dynamics in estimating net primary productivity for potential vegetation in North America. Global Biogeochemical Cycles 6, 101–124.

Mo, X., Chen, J.M., Ju, W., Black, T.A., 2008. Optimization of ecosystem model parameters through assimilating eddy covariance flux data with an ensemble Kalman filter. Ecological Modelling 217, 157–173.

Monson, R.K., Turnipseed, A.A., Sparks, J.P., Harley, P.C., Scott-Denton, L.E., Sparks, K.L., Huxman, T.E., 2002. Carbon sequestration in a high-elevation, subalpine forest. Global Change Biology 8, 459–478.

Nemani, R.R., Keeling, C.D., Hashimoto, H., et al., 2003. Climate-driven increases in global terrestrial net primary production from 1982 to 1999. Science 300, 1560–1563.

Parton, W.J., Scurlock, J.M.O., Ojima, D.S., Gilmanov, T.G., Scholes, R.J., et al., 1993. Observations and modeling of biomass and soil organic matter dynamics for the grassland biome worldwide. Global Biogeochemical Cycles 7, 785–809.

Pietsch, S.A., Hasenauer, H., 2006. Evaluating the self-initialization procedure for large-scale ecosystem models. Global Change Biology 12, 1658–1669.

Potter, C.S., Randerson, J.T., Field, C.B., Matson, P.A., Vitousek, P.M., et al., 1993. Terrestrial ecosystem production: a process model based on global satellite and surface data. Global Biogeochemical Cycles 7, 811–841.

Press, W.H., Teukolsky, S.A., Vetterling, W.T., Flannery, B.P., 1992. Numerical Recipes: The Art of Scientific Computing, second ed. Cambridge University Press, 994 pp.

Raich, J.W., Rastetter, E.B., Melillo, J.M., Kicklighter, D.W., Steudler, P.A., et al., 1991. Potential net primary productivity in South America: application of a global model. Ecological Applications 1, 399–429.

Randerson, J.T., Thompson, M.V., Conway, T.J., Fung, I.Y., Field, C.B., 1997. The contribution of terrestrial sources and sinks to trends in the seasonal cycle of atmospheric carbon dioxide. Global Biogeochemical Cycles 11, 535–560.

Raupach, M.R., Rayner, P.J., Barrett, D.J., Defries, R.S., Heimann, M., Ojima, D.S., Quegan, S., Schmullius, C.C., 2005. Model-data synthesis in terrestrial carbon observation: methods, data requirements and data uncertainty specifications. Global Change Biology 11, 378–397.

Running, S.W., Coughlan, J.C., 1988. A general model of forest ecosystem processes for regional applications: I. Hydrologic balance, canopy gas exchange and primary production processes. Ecol. Model. 42, 125–154.

Running, S.W., Gower, S.T., 1991. Forest-BGC, a general model of forest ecosystem processes for regional applications: II. Dynamic carbon allocation and nitrogen budgets. Tree Physiology 9, 147–160.

Sellers, P.J., Dickinson, R.E., Randall, D.A., et al., 1997. Modeling the exchanges of energy, water, and carbon between continents and the atmosphere. Science 275, 502–509.

Schimel, D., Melillo, J., Tian, H., McGuire, A.D., Kicklighter, D., et al., 2000. Contribution of increasing CO_2 and climate to carbon storage by ecosystems of the United States. Science 287, 2004–2006.

Schmid, H.P., Grimmond, C.S.B., Cropley, F., Offerle, B., Su, H.-B., 2000. Measurements of CO_2 and energy fluxes over a mixed hardwood forest in the Midwestern United States. Agricultural and Forest Meteorology 103, 355–373.

Schwarz, P.A., Law, B.E., Williams, M., Irvine, J., Kurpius, M., Moore, D., 2004. Climatic versus biotic constraints on carbon and water fluxes in seasonally drought-affected ponderosa pine ecosystems. Global Biogeochemical Cycles 18, doi:10.1029/2004GB002234.

Thornton, P.E., Running, S.W., White, M.A., 1997. Generating surfaces of daily meteorology variables over large regions of complex terrain. Journal of Hydrology 190, 214–251.

Thornton, P.E., 1998. Description of a numerical simulation model for predicting the dynamics of energy, water, carbon, and nitrogen in a terrestrial ecosystem. Ph.D. dissertation, University of Montana, Missoula, MT, 280 pp. [Available from Mansfield Library, University of Montana, Missoula, MT 59812.].

Thornton, P.E., Law, B.E., Gholz, H.L., Clark, K.L., Falge, E., et al., 2002. Modeling and measuring the effects of disturbance history and climate on carbon and water budgets in evergreen needleleaf forests. Agricultural and Forest Meteorology 113, 185–222.

Thornton, P.E., Rosenbloom, N.A., 2005. Ecosystem model spin-up: Estimating steady state conditions in a coupled terrestrial carbon and nitrogen cycle model. Ecological Modelling 189, 25–48.

Turnipseed, A.A., Blanken, P.D., Anderson, D.E., Monson, R.K., 2002. Energy budget above a high-elevation subalpine forest in complex topography. Agricultural and Forest Meteorology 110, 117–201.

Wang, Y.-P., Leuning, R., Cleugh, H.A., Coppin, P.A., 2001. Parameter estimation in surface exchange models using nonlinear inversion: how many parameters can we estimate and which measurements are most useful? Global Change Biology 7, 495–510.

Wang, Y.-P., Baldocchi, D., Leuning, R., Falge, E., Vesala, T., 2006. Estimating parameters in a land-surface model by applying nonlinear inversion to eddy covariance flux measurements from eight FLUXNET sites. Global Change Biology 12, 1–19.

Waring, R.H., Running, S.W., 1998. Forest ecosystems: analysis at multiple scales, second ed. Academic Press, 370 pp.

White, M.A., Thornton, P.E., Running, S.W., Nemani, R.R., 2000. Parameterization and sensitivity analysis of the Biome-BGC terrestrial ecosystem model: net primary production controls. Earth Interactions 4 (3), 1–85.

Williams, M., Schwarz, P.A., Law, B.E., Irvine, J., Kurpius, M.R., 2005. An improved analysis of forest carbon dynamics using data assimilation. Global Change Biology 11, 89–105.

Yang, F., White, M.A., Michaelis, A., Ichii, K., Hashimoto, H., et al., 2006. Prediction of continental scale evapotranspiration by combining MODIS and AmeriFlux data through Support Vector Machine. IEEE Transactions on Geoscience and Remote Sensing 44, 3452–3461.